Cosmic strings: a decade in the gravitational wave era

Pierre Auclair

TUG 2025

Cosmology, Universe and Relativity at Louvain (CURL)
Institute of Mathematics and Physics
Louvain University, Louvain-la-Neuve, Belgium

(Soon in IAP, Paris)

Introduction to cosmic strings

What is a cosmic string ?

Cosmic string

A cosmic string is a one dimensional topological defect[1]. May form when the vacuum manifold has non-contractible loops.

Example: Mexican hat potential

- Vacuum manifold is a circle $\mathcal{M} = S^1$
- Fundamental group $\Pi_1(\mathcal{M}) = \mathbb{Z}$
- We expect strings to be formed in most models of spontaneous symmetry breaking[2]

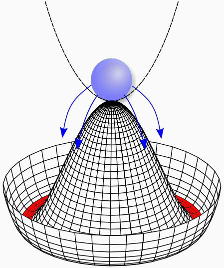

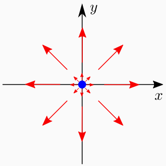

[1] Kibble 1976
[2] Jeannerot, Rocher, and Sakellariadou 2003

Cosmic string evolution

Energy scale	Width	Linear density
GUT : 10^{16} GeV	2×10^{-32} m	$G\mu \approx 10^{-6}$
3×10^{10} GeV	5×10^{-27} m	$G\mu \approx 10^{-17}$
10^{8} GeV	2×10^{-24} m	$G\mu \approx 10^{-22}$
EW : 100 GeV	2×10^{-18} m	$G\mu \approx 10^{-34}$

Nambu-Goto strings: one dimensional limit

- Width of the string very small compared to other length scales in the problem.
- String modeled as a line with mass per unit length $\mu \propto \eta^2$
- The Nambu-Goto action which minimizes the area swept by the string

$$\mathcal{S} = -\mu \int \mathrm{d}\tau\, \mathrm{d}\sigma \sqrt{-\det \gamma}$$

γ_{ab}: the induced metric on the string, τ is a time-like and σ a space-like coordinate along the string

Nambu-Goto strings in flat spacetime

Cosmic string dynamics

In flat spacetime, it satisfies a wave equation whose solution is

$$\mathbf{X}(t,\sigma) = \frac{1}{2}[\mathbf{a}(t-\sigma) + \mathbf{b}(t+\sigma)], \quad \mathbf{a}'^2 = \mathbf{b}'^2 = 1.$$

For a closed loop $\mathbf{X}(t,\sigma+\ell) = \mathbf{X}(t,\sigma)$: it oscillates with a period $T = \frac{\ell}{2}$.

Cosmic strings emit gravitational waves:

- Oscillation

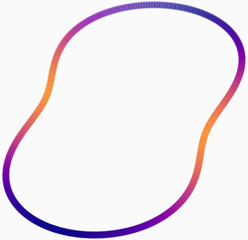

Nambu-Goto strings in flat spacetime

Cosmic string dynamics

In flat spacetime, it satisfies a wave equation whose solution is

$$\mathbf{X}(t,\sigma) = \frac{1}{2}[\mathbf{a}(t-\sigma) + \mathbf{b}(t+\sigma)], \quad \mathbf{a}'^2 = \mathbf{b}'^2 = 1.$$

For a closed loop $\mathbf{X}(t,\sigma+\ell) = \mathbf{X}(t,\sigma)$: it oscillates with a period $T = \frac{\ell}{2}$.

Cosmic strings emit gravitational waves:

- Oscillation
- Kink: when $\mathbf{X}'$ is not continuous

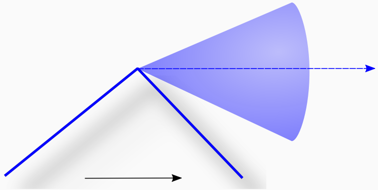

Nambu-Goto strings in flat spacetime

Cosmic string dynamics

In flat spacetime, it satisfies a wave equation whose solution is

$$\mathbf{X}(t,\sigma) = \frac{1}{2}[\mathbf{a}(t-\sigma) + \mathbf{b}(t+\sigma)], \quad \mathbf{a}'^2 = \mathbf{b}'^2 = 1.$$

For a closed loop $\mathbf{X}(t,\sigma+\ell) = \mathbf{X}(t,\sigma)$: it oscillates with a period $T = \frac{\ell}{2}$.

Cosmic strings emit gravitational waves:

- Oscillation
- Kink: when $\mathbf{X}'$ is not continuous
- Kink-kink collision

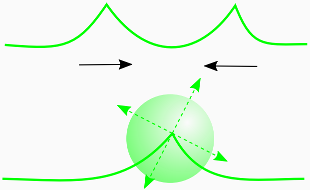

Nambu-Goto strings in flat spacetime

Cosmic string dynamics

In flat spacetime, it satisfies a wave equation whose solution is

$$\mathbf{X}(t,\sigma) = \frac{1}{2}[\mathbf{a}(t-\sigma) + \mathbf{b}(t+\sigma)], \quad \mathbf{a}'^2 = \mathbf{b}'^2 = 1.$$

For a closed loop $\mathbf{X}(t,\sigma+\ell) = \mathbf{X}(t,\sigma)$: it oscillates with a period $T = \frac{\ell}{2}$.

Cosmic strings emit gravitational waves:

- Oscillation
- Kink: when $\mathbf{X}'$ is not continuous
- Kink-kink collision
- Cusp: when $\dot{\mathbf{X}}^2 = 1$

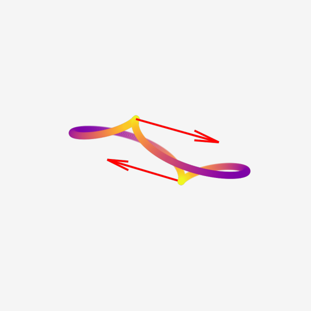

Nambu-Goto strings in flat spacetime

Cosmic string dynamics

In flat spacetime, it satisfies a wave equation whose solution is

$$\mathbf{X}(t,\sigma) = \frac{1}{2}[\mathbf{a}(t-\sigma) + \mathbf{b}(t+\sigma)], \quad \mathbf{a}'^2 = \mathbf{b}'^2 = 1.$$

For a closed loop $\mathbf{X}(t,\sigma+\ell) = \mathbf{X}(t,\sigma)$: it oscillates with a period $T = \frac{\ell}{2}$.

Cosmic strings emit gravitational waves:

- Oscillation
- Kink: when $\mathbf{X}'$ is not continuous
- Kink-kink collision
- Cusp: when $\dot{\mathbf{X}}^2 = 1$

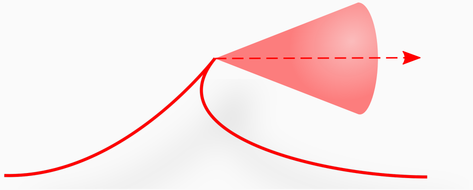

Signature in terms of gravitational waves (GW)

The waveform of the gravitational wave arriving at the detector is known[1] and looked for in GW detectors

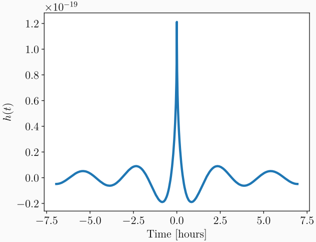

[1] Vachaspati and Alexander Vilenkin 1985; Damour and Alexander Vilenkin 2000.

Signature in terms of gravitational waves (GW)

The waveform of the gravitational wave arriving at the detector is known[1] and looked for in GW detectors

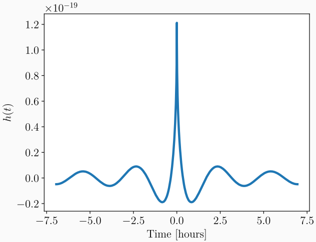

The uncorrelated sum of all the GW signals produced by cosmic string loops constitutes a Stochastic Background of GW.

$$\Omega_{\mathrm{GW}}(\ln f) = \frac{1}{\rho_c}\frac{\mathrm{d}\rho_{\mathrm{GW}}}{\mathrm{d}\ln f}$$

[1] Vachaspati and Alexander Vilenkin 1985; Damour and Alexander Vilenkin 2000.

Number of cosmic string loops $\mathcal{N}(\ell, t)$

Continuity equation for the loop distribution

$$\frac{\partial}{\partial t}\left(a^3 \mathcal{N}\right) + \frac{\partial}{\partial \ell}\left(\frac{\mathrm{d}\ell}{\mathrm{d}t}\ a^3 \mathcal{N}\right) = a^3(t)\ \mathcal{P}(\ell, t)$$

Number of cosmic string loops $\mathcal{N}(\ell, t)$

Continuity equation for the loop distribution

$$\frac{\partial}{\partial t}(a^3\mathcal{N}) + \frac{\partial}{\partial \ell}\left(\frac{\mathrm{d}\ell}{\mathrm{d}t}\, a^3\mathcal{N}\right) = a^3(t)\boxed{\mathcal{P}(\ell, t)}$$

Loop production function

- One-scale model Kibble 1985

$$t^5\mathcal{P}(\ell, t) = C\delta\left(\frac{\ell}{t} - \alpha\right)$$

- VOS model Martins and Shellard 1996
- CVOS model Auclair, Blasi, et al. 2023

$$t^5\mathcal{P}(\ell, t) = C\delta\left[\frac{\ell}{t} - \alpha(t)\right]$$

- Power-law loop production function Lorenz, Ringeval, and Sakellariadou 2010; Auclair, Ringeval, et al. 2019

$$t^5\mathcal{P}(\ell, t) = C\left(\frac{\ell}{t}\right)^{2\chi-3}$$

Number of cosmic string loops $\mathcal{N}(\ell, t)$

Continuity equation for the loop distribution

$$\frac{\partial}{\partial t}(a^3\mathcal{N}) + \frac{\partial}{\partial \ell}\left(\frac{\mathrm{d}\ell}{\mathrm{d}t}a^3\mathcal{N}\right) = a^3(t)\ \mathcal{P}(\ell, t)$$

Decay rate

- $\mathrm{d}\ell/\mathrm{d}t = -\Gamma G\mu$ A. Vilenkin 1981
- Energy lost to cusps J. J. Blanco-Pillado and Olum 1999
- Energy lost to kinks Matsunami et al. 2019; Hindmarsh, Lizarraga, et al. 2021
- $\mathrm{d}\ell/\mathrm{d}t = -\mathcal{J}(\ell)\Gamma G\mu$ Auclair, Steer, and Vachaspati 2020
- Multiple populations Hindmarsh and Kume 2023 $\Omega_{\mathrm{gw}}^{(\mathrm{AH})} = f_{\mathrm{NG}}\Omega_{\mathrm{gw}}^{(\mathrm{NG})}$

GW constraints on vanilla cosmic string models

Constraints on Cosmic Strings Using Data from the Third Advanced LIGO–Virgo Observing Run

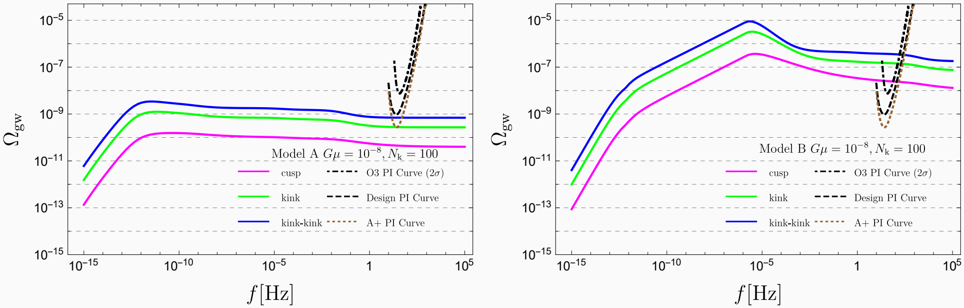

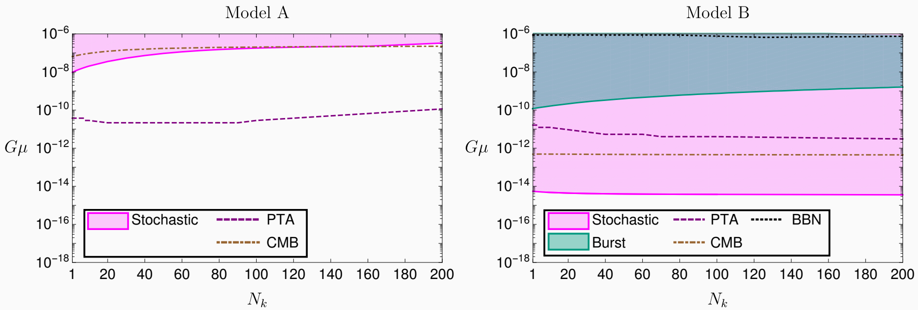
Model A
Model B
$G\mu$
N_k
Stochastic
PTA
CMB
Burst
BBN
10^{-6}
10^{-8}
10^{-10}
10^{-12}
10^{-14}
10^{-16}
10^{-18}
1 20 40 60 80 100 120 140 160 180 200

Scenarios / Interpretations of the PTA signal

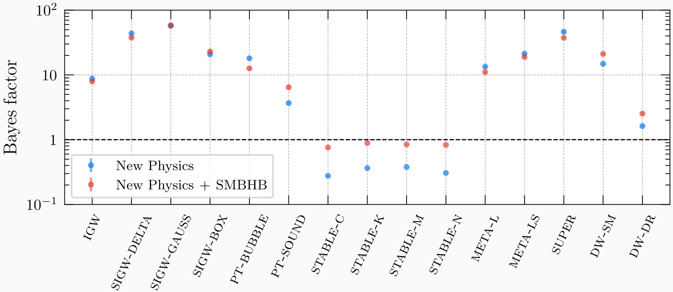

Figure: Bayes factors for NANOGRAV 15 years Credits: Afzal et al. 2023

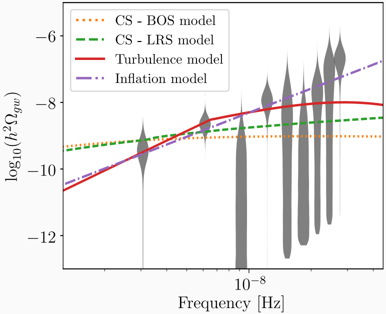

Figure: EPTA Credits: Antoniadis et al. 2023

- First-order phase transitions (PT)
- Cosmic strings (STABLE/META/SUPER)
- Domain walls (DW)
- Inspiraling supermassive black hole binaries (SMBHBs)
- Scalar-induced GWs (SIGW)

Future constraints on cosmic strings from GWs

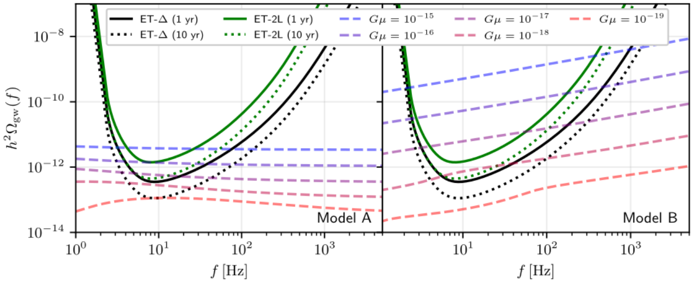

Figure 2.14: Forecast power-law-integrated GWB sensitivity of ET, compared with signals from local Nambu-Goto strings of various tensions $G\mu$. We consider both the triangular configuration for ET with 10 km arms, and the 2L configuration with 15 km arms, misaligned as in [16]; the solid black curves corresponds to one year of observations, while the dotted black curve corresponds to 10 years. The left and right panels show the predictions for models A [814] and B [815] of the loop network, respectively. Both models predict that, in the triangle configuration, ET will be sensitive to $G\mu \gtrsim 10^{-18}$ after one year of observations with SNR ≥ 1.

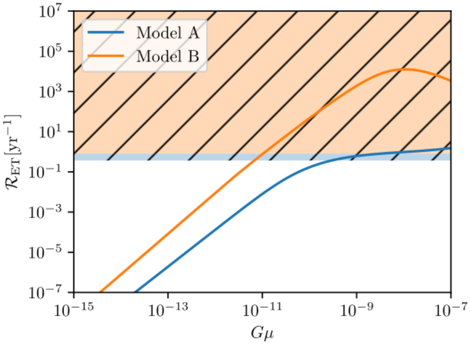

Figure 2.16: Expected rate of detected bursts in Einstein Telescope as a function of the string tension for models A and B. In case ET does not detect bursts from cosmic string cusps, the orange hatched region is excluded after 4 years of observations and the blue hatched region is excluded after 8 years.

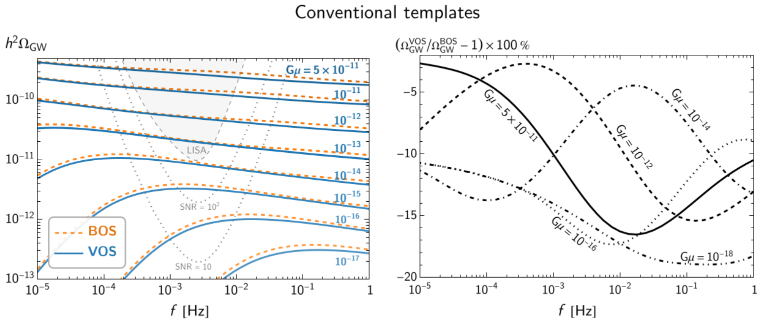

Figure 3. *Left Panel:* GWB spectra from a local cosmic string network for $G\mu = 5\times 10^{-11}, 10^{-11}, 10^{-12}, ..., 10^{-18}$, obtained using the VOS model (Sect. 3.1, solid blue) and the BOS model (Sect. 3.2, dashed orange). The g_*, g_{*s} evolutions correspond to Saikawa-Shirai [185]. The top gray dotted line is the LISA (AA-channel) noise sensitivity, while the other two gray lines are the PLS curves with SNR = 100 and 10, respectively, and with $T_{\rm obs} = 75\% \times 4 = 3$ years (see Eq. (5.6) for LISA PLS curve definition). *Right Panel:* The % relative difference of the predictions from the VOS and BOS modelings, for different tensions $G\mu$. Note that $\Omega_{\rm GW}^{\rm VOS}(f) < \Omega_{\rm GW}^{\rm BOS}(f)$ for all LISA frequencies.

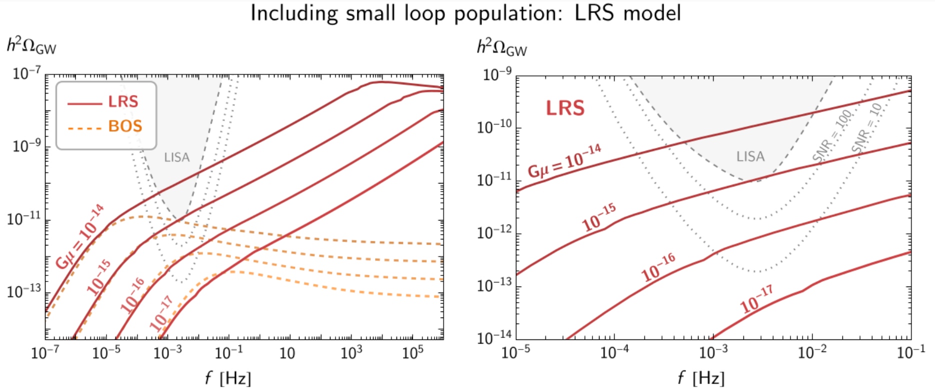

Figure 5. GWB spectra from the LRS model (discussed in Section 4.1.1) of different $G\mu$ are shown in red, in comparison to the GWB spectra from the BOS model in dashed orange (which includes de running of g_*, g_{*s}, contrary to the LRS modeling). The LRS spectra have their high-frequency part enhanced by the existence of small-loop populations.

Motivations

- New observational signature in LISA, complementary to other detectors
- Impact of repetitions on sky-localization and parameter reconstruction

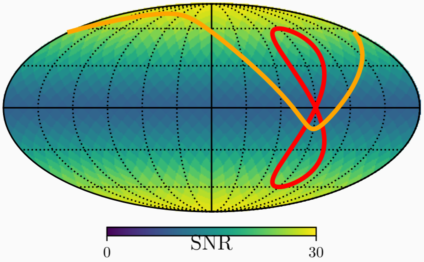

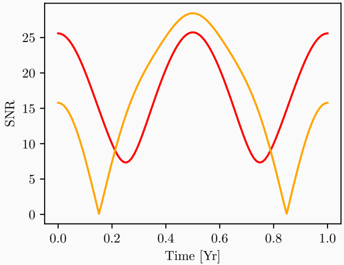

Is fragmentation important?

- Family of artificial loops with no angular momentum
- Loops fragment significantly
- Stable loops are ≈ squares with angular momentum

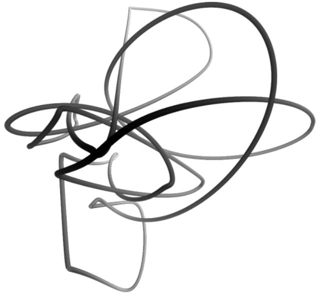

FIG. 2. A sample initial loop with 10 harmonic modes. The darker, thicker segments of the loop are nearer the viewer.

- Family of artificial loops with no angular momentum
- Loops fragment significantly
- Stable loops are ≈ squares with angular momentum

Source	Segments	Modes (M)	Initial Loops (N)	Stable Loops
SP	128[a]	10	20	561
CA	600[b]	10	200	5,723
Present work	10,000	3	1,000	8,308
—	10,000	10	3,000	94,628
—	10,000	20	1,000	63,490
—	10,000	30	1,000	96,207
—	10,000	40	1,000	128,764
—	10,000	50	1,000	157,968
—	50,000	10	1,000	32,158
—	50,000	50	1,000	162,157

[a] Loops were also run with 256 segments without producing significantly more small loops
[b] The loops were rerun with 800 segments resulting in almost no new daughter loops being produced.

TABLE I. Parameters from studies of loop fragmentation. Modes refers to M in Eq. (4). The numbers provided here are for the "Type A" loops defined by SP and used by CA; see the discussion after Eq. (4) for more details. For SP see [2] and for CA see [4].

- Family of artificial loops with no angular momentum
- Loops fragment significantly
- Stable loops are ≈ squares with angular momentum

Question?

- Realistic loops?
- Expanding background?
- Typical fragmentation scale?
- Scaling with time?

Source	Segments	Modes (M)	Initial Loops (N)	Stable Loops
SP	128[a]	10	20	561
CA	600[b]	10	200	5,723
Present work	10,000	3	1,000	8,308
—	10,000	10	3,000	94,628
—	10,000	20	1,000	63,490
—	10,000	30	1,000	96,207
—	10,000	40	1,000	128,764
—	10,000	50	1,000	157,968
—	50,000	10	1,000	32,158
—	50,000	50	1,000	162,157

[a] Loops were also run with 256 segments without producing significantly more small loops

[b] The loops were rerun with 800 segments resulting in almost no new daughter loops being produced.

TABLE I. Parameters from studies of loop fragmentation. Modes refers to M in Eq. (4). The numbers provided here are for the "Type A" loops defined by SP and used by CA; see the discussion after Eq. (4) for more details. For SP see [2] and for CA see [4].

$$\frac{\partial n}{\partial t} = -n(\ell,t)\frac{\partial \dot{\ell}}{\partial \ell} - \frac{\partial n(\ell,t)}{\partial \ell}\dot{\ell} + \lim_{\ell \to 0^+}\left[n(\ell,t)\dot{\ell}\right]\delta(\ell) - 3Hn(\ell,t) \tag{2.9}$$

$$+ \int_0^{\ell/2} A(\ell;\ell',\ell-\ell')n(\ell',t)n(\ell-\ell',t)d\ell' \quad \leftarrow \text{Term 1} \tag{2.10}$$

$$+ \int_\ell^{\infty} B(\ell,\ell'-\ell;\ell')n(\ell',t)d\ell' \quad \leftarrow \text{Term 2} \tag{2.11}$$

$$- \; n(\ell,t)\int_0^{\infty} A(\ell+\ell';\ell,\ell')n(\ell',t)d\ell' \quad \leftarrow \text{Term 3} \tag{2.12}$$

$$- \; n(\ell,t)\int_0^{\ell/2} B(\ell',\ell-\ell';\ell)d\ell' \quad \leftarrow \text{Term 4.} \tag{2.13}$$

Figure: Rate equation including collisions and fragmentations of loops

The evolution of a network of cosmic string loops

Copeland, Kibble, Steer (1998)

Firstly suppose that $\xi \ll y \ll \ell/2$. On these scales the loop is, by assumption, a Brownian random walk, and we take B to be given by

$$B(\ell - y, y; \ell) = \frac{\tilde{\chi}\ell}{(\bar{\xi}y)^{3/2}} \qquad \left(\frac{\ell}{2} \gg y \gg \bar{\xi}\right), \tag{3.3}$$

where $\tilde{\chi}$ is another relative velocity. To obtain equation (3.3), consider one of the $\bar{\xi}$ segments of the loop, and another such segment $m = y/\bar{\xi}$ steps away. Then the straight critical value of c was found to depend on a ratio of parameters of the model (9.3.3). In an expanding universe we were also able to make some predictions for how we believe a network of cosmic string loops might evolve. We suggested that either the loops disappear, or that infinite strings are formed (section 9.4). These results may prove interesting in light of the problems with the standard cosmic string scenario of structure formation [2]. However, due to the complicated nature of the rate equation, we have been unable to verify our predictions by a numerical solution. The reasons for this were indicated in section 9.5.

Figure: Final lines of Danièle Steer's PhD thesis

Nambu-Goto simulations

- Loops are objects
- Fragmentations/collisions are events
- Can we store and use this information?

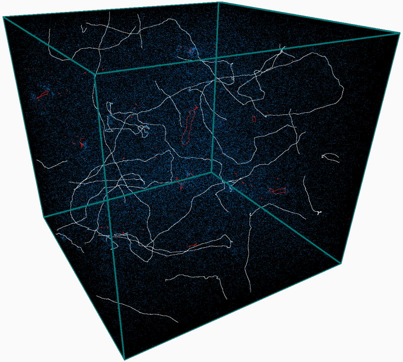

Nambu-Goto simulations with a new twist

(Preliminary)

Nambu-Goto simulations

- Loops are objects
- Fragmentations/collisions are events
- Can we store and use this information?

```
[40]: fragmentations
```

[40]:

	ISTEP	LABOLD	LABOLD.1	LABEL1	LABEL3	LGTHI1	LGTHI3	TIMEXCHG	ENER OLD	ENER NEW/OLD	ENER NEW
0	1	1	1	20535	20536	100	6508588	0.070408	3232.583000	0.049670	3232.533000
1	1	20536	20536	20537	20538	4600	6503988	0.070399	3232.140000	2.284179	3229.856000
2	1	20538	20538	20539	20540	4077	6499911	0.070525	3235.652000	2.027834	3233.624000
3	1	20540	20540	20541	20542	101	6499810	0.070498	3232.357000	0.049828	3232.307000
4	1	20542	20542	20543	20544	20444	6479366	0.070483	3231.610000	10.163510	3221.446000
...	...	...	...	...	...	...	...	...	...	...	...
9581	28586	5768321	5768321	5768322	5768323	1	1	1.000014	0.003182	0.001151	0.002031
9582	28586	5768322	5768322	5768324	5768325	1	1	1.000032	0.001151	0.000713	0.000438
9583	28586	5768323	5768323	5768326	5768327	1	1	1.000020	0.002031	0.000509	0.001522
9584	28586	5768326	5768326	5768328	5768329	1	1	1.000025	0.000509	0.000226	0.000283
9585	28586	5768277	5768277	5768330	5768331	5	15	0.999974	0.016142	0.003813	0.012328

2766071 rows × 11 columns

```
[41]: collisions
```

[41]:

	ISTEP	LABOLD	LABOLD.1	LABEL1	LABEL3	LGTHI1	LGTHI3	TIMEXCHG	ENER OLD	ENER NEW/OLD	ENER NEW
16	1	20566	20562	20567	20567	3794487	2676618	0.070453	1885.784000	1330.204000	3215.9880
23	1	20579	20572	20580	20580	2243018	1995975	0.070477	1115.060000	992.315400	2107.3760
28	1	20588	20577	20589	20589	1238993	2231363	0.070475	615.903900	1109.306000	1725.2100
29	1	20587	20589	20590	20590	2997384	3470356	0.070478	1490.176000	1725.270000	3215.4460
38	1	20606	20602	20607	20607	833480	5628405	0.070489	414.421400	2798.631000	3213.0530
...	...	...	...	...	...	...	...	...	...	...	...
9457	28571	5767930	5768076	5768079	5768079	12	285240	0.999664	0.009282	228.209900	228.2192
9471	28573	5767880	5768099	5768106	5768106	20	254436	0.999709	0.015755	203.619000	203.6347
9481	28575	5768107	5767724	5768125	5768125	254442	16	0.999747	203.624800	0.007147	203.6320
9505	28578	5768132	5768131	5768172	5768172	254431	21	0.999781	203.607200	0.016843	203.6241
9533	28580	5768191	5767654	5768227	5768227	285189	16	0.999844	228.176700	0.012992	228.1897

215655 rows × 11 columns

Nambu-Goto simulations

- Loops are objects
- Fragmentations/collisions are events
- Can we store and use this information?

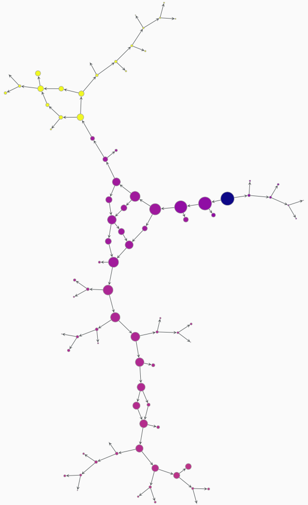

Nambu-Goto simulations with a new twist (Preliminary)

Nambu-Goto simulations

- Loops are objects
- Fragmentations/collisions are events
- Can we store and use this information?

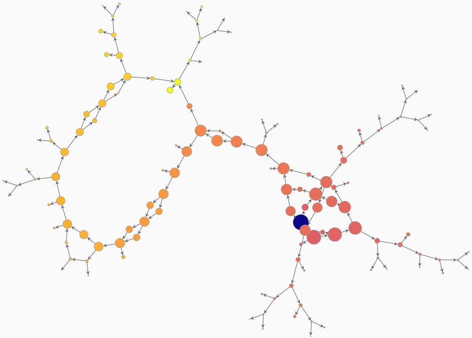

Fragmentation in Nambu-Goto simulations (Preliminary)

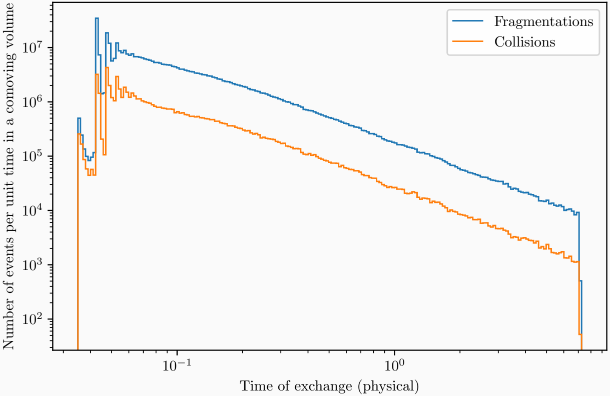

Fragmentation in Nambu-Goto simulations (Preliminary)

Fragmentation in Nambu-Goto simulations

(Preliminary)

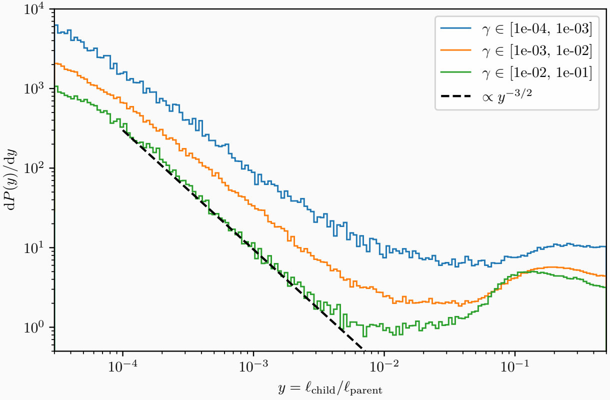

A model of cosmic string loop fragmentation

Copeland et al. 1998 but...

- No collisions $\mathcal{A} = 0$
- Only sub-Hubble loops $\Longrightarrow$ loop production function
- Simplified ansatz for the fragmentation function $\mathcal{B}$

$$
\begin{aligned}
\frac{\partial n}{\partial t} &= -n(\ell,t)\frac{\partial \dot{\ell}}{\partial \ell} - \frac{\partial n(\ell,t)}{\partial \ell}\dot{\ell} + \lim_{\ell\to 0^+}\left[n(\ell,t)\dot{\ell}\right]\delta(\ell) - 3Hn(\ell,t) && (2.9)\\
&+ \int_0^{\ell/2} A(\ell;\ell',\ell-\ell')n(\ell',t)n(\ell-\ell',t)d\ell' \quad \leftarrow \text{Term 1} && (2.10)\\
&+ \int_\ell^{\infty} B(\ell,\ell'-\ell;\ell')n(\ell',t)d\ell' \quad \leftarrow \text{Term 2} && (2.11)\\
&- n(\ell,t)\int_0^{\infty} A(\ell+\ell';\ell,\ell')n(\ell',t)d\ell' \quad \leftarrow \text{Term 3} && (2.12)\\
&- n(\ell,t)\int_0^{\ell/2} B(\ell',\ell-\ell';\ell)d\ell' \quad \leftarrow \text{Term 4.} && (2.13)
\end{aligned}
$$

Copeland et al. 1998 but...

- No collisions $\mathcal{A} = 0$
- Only sub-Hubble loops $\implies$ loop production function
- Simplified ansatz for the fragmentation function $\mathcal{B}$

$$\mathcal{B}(y > \xi, \ell - y; \ell) = \frac{\chi \ell}{(\xi y)^{3/2}} \Theta(y - \xi) + \frac{\chi \ell}{\xi^3} \left(\frac{y}{\xi}\right)^{\sigma} \Theta(\xi - y) \, .$$

New Boltzmann equation - linear Integro-Differential Equation (IDE):

$$\frac{\partial}{\partial t}\left[a^3(t)\mathcal{N}\right] + \frac{\partial}{\partial \ell}\left[\dot{\ell} a^3(t)\mathcal{N}\right] = a^3(t)\mathcal{P}(t,\ell) - a^3(t)\mathcal{N}(t,\ell)\int_{\xi}^{\ell/2} \mathcal{B}(y,\ell)\,\mathrm{d}y$$
$$+ a^3(t)\int_{2\ell}^{\alpha t} \mathcal{B}(\ell, L)\mathcal{N}(t,L)\,\mathrm{d}L + a^3(t)\int_{\ell}^{2\ell} \mathcal{B}(L-\ell, L)\mathcal{N}(t,L)\,\mathrm{d}L \, .$$

- Fragmentation rate = decay time

$$\tau^{-1} = \int_{\xi}^{\ell/2} \mathcal{B}(y,\ell)\,\mathrm{d}y$$

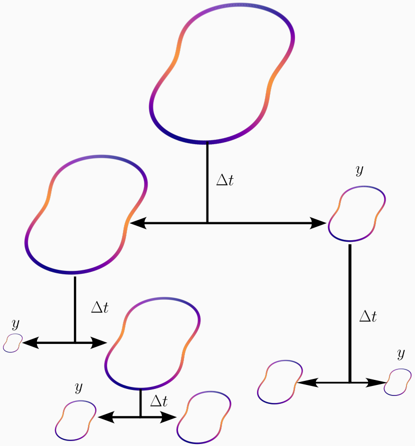

- Fragmentation rate = decay time

$$\tau^{-1} = \int_{\xi}^{\ell/2} \mathcal{B}(y,\ell)\,\mathrm{d}y$$

- Probability to be still alive

$$G(t) = \exp\left[-\int_{t_\star}^{t} \tau^{-1}\,\mathrm{d}t\right]$$

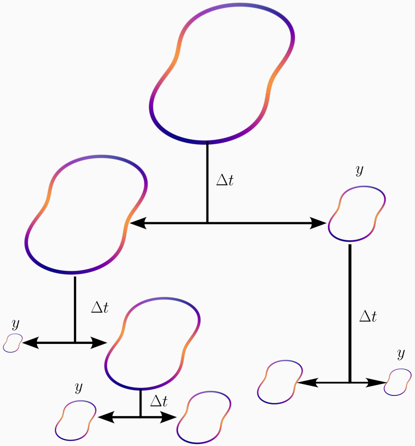

- Fragmentation rate = decay time

$$\tau^{-1} = \int_{\xi}^{\ell/2} \mathcal{B}(y,\ell)\,\mathrm{d}y$$

- Probability to be still alive

$$G(t) = \exp\left[-\int_{t_\star}^{t} \tau^{-1}\,\mathrm{d}t\right]$$

- Lifetime

$$\Delta t = G^{-1}(X),\; X \in \mathcal{U}(0,1)$$

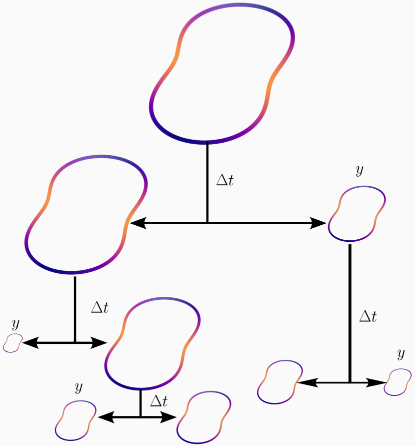

- Fragmentation rate = decay time

$$\tau^{-1} = \int_{\xi}^{\ell/2} \mathcal{B}(y,\ell)\,\mathrm{d}y$$

- Probability to be still alive

$$G(t) = \exp\left[-\int_{t_\star}^{t} \tau^{-1}\,\mathrm{d}t\right]$$

- Lifetime

$$\Delta t = G^{-1}(X),\ X \in \mathcal{U}(0,1)$$

- The size of the fragmented loop y satisfies

$$\int_0^x \mathcal{B}(y,\ell)\,\mathrm{d}y = X \int_0^{\ell/2} \mathcal{B}(y,\ell)\,\mathrm{d}y\,,\ X \in \mathcal{U}(0,1)$$

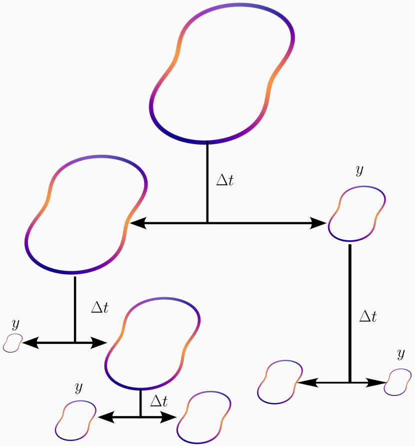

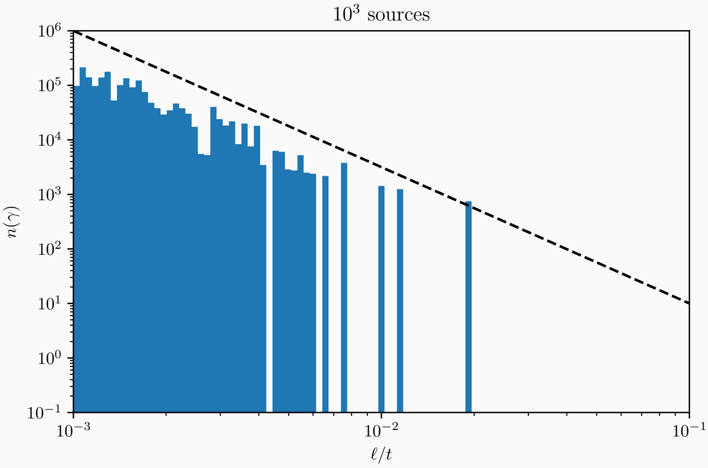
10^3 sources
10^6
10^5
10^4
10^3
10^2
10^1
10^0
10^{-1}
$n(\gamma)$
10^{-3}
10^{-2}
10^{-1}
ℓ/t

Unconnected Loop Model (ULM) – does it work?

2508.11596

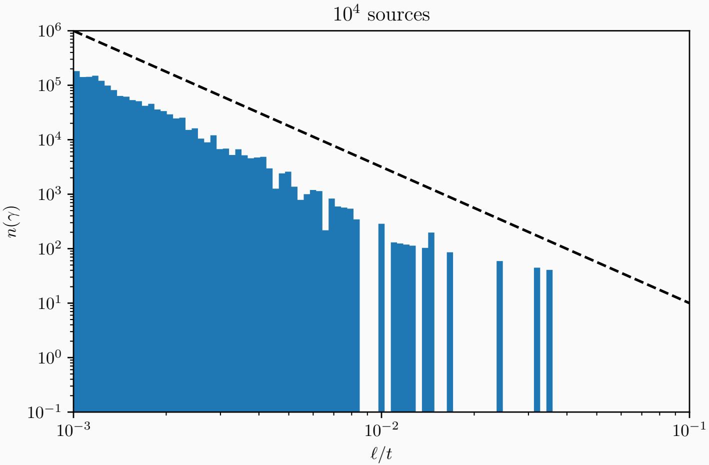

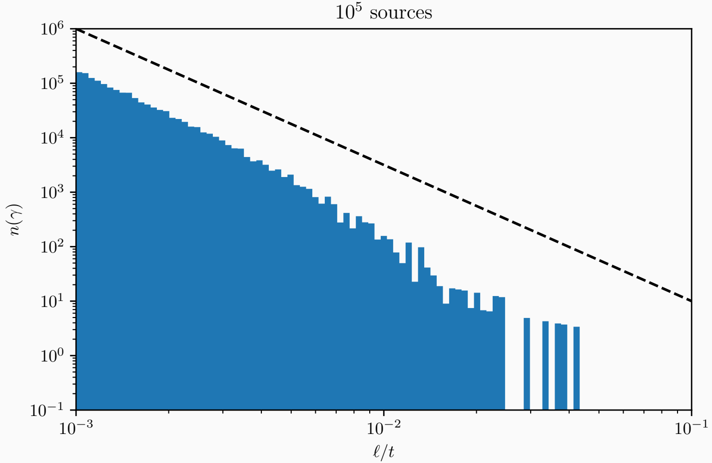
10^5 sources
$n(\gamma)$
10^6
10^5
10^4
10^3
10^2
10^1
10^0
10^{-1}
10^{-3}
10^{-2}
10^{-1}
ℓ/t

Unconnected Loop Model (ULM) – does it work?

2508.11596

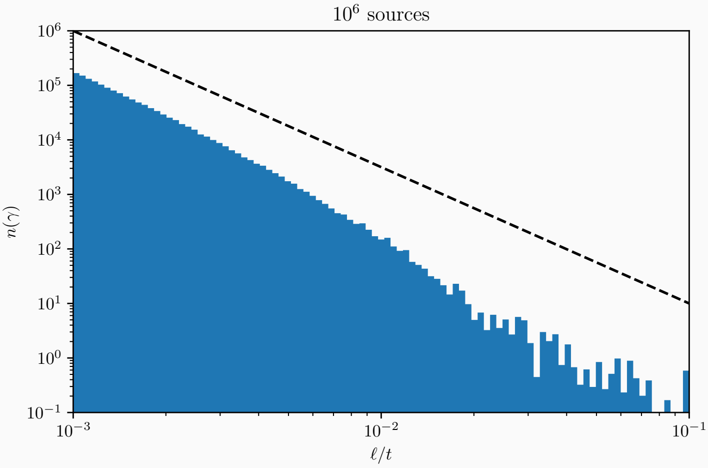

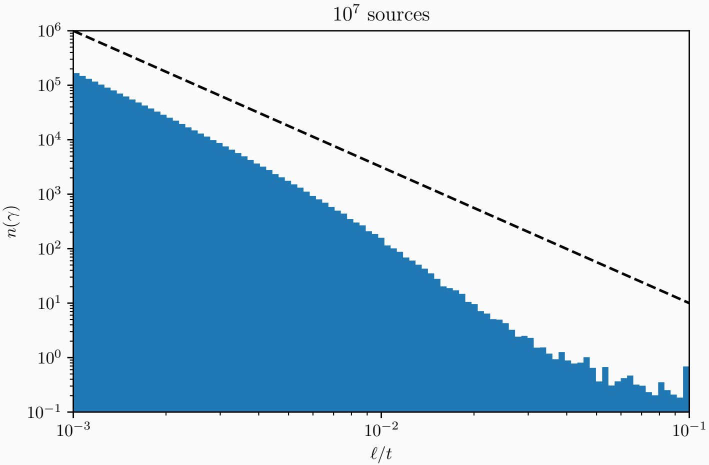
10^7 sources
10^6
10^5
10^4
10^3
10^2
10^1
10^0
10^−1
n(γ)
10^−3
10^−2
10^−1
ℓ/t

Unconnected Loop Model (ULM) – does it work?

2508.11596

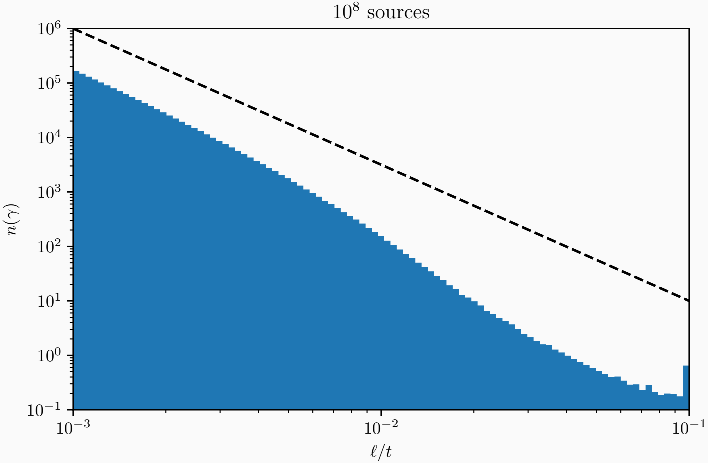

Scaling units: $\gamma = \ell/t$ and $n(\gamma) = t^4\mathcal{N}(\ell,t)$

$$\Gamma G\mu \frac{\mathrm{d}n}{\mathrm{d}\gamma} - (3\nu - 4)n(\gamma) - n(\gamma)\int_{\xi}^{\gamma/2} \frac{\chi\gamma}{(\xi_c z)^{3/2}}\,\mathrm{d}z = -C\delta(\gamma-\alpha)$$
$$-\int_{2\gamma}^{\alpha} \frac{\chi}{(\xi_c\gamma)^{3/2}} n(Z)\,\mathrm{d}Z - \int_{\gamma}^{2\gamma} \frac{\chi Z}{[\xi_c(Z-\gamma)]^{3/2}} n(Z)\,\mathrm{d}Z\ .$$

Technical details

- Intermediate integrals
- Boundary at α
- Adaptative steps: convergence and integral reconstruction
- Solve for $\ln n(\gamma)$
- Implicit scheme $\to W_{-1}(x)$

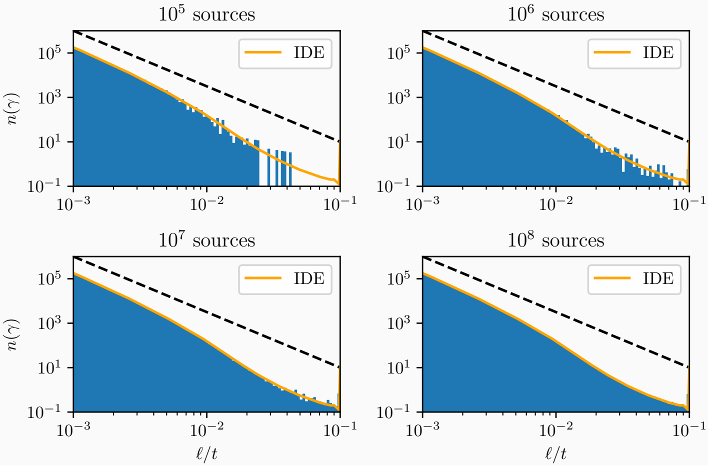
10^5 sources
10^6 sources
10^7 sources
10^8 sources
IDE
$n(\gamma)$
ℓ/t
10^5
10^3
10^1
10^{-1}
10^{-3}
10^{-2}
10^{-1}

Comparison between the two methods

ULM

- Parallelisable
- Not manifestly scaling
- Accurate on small scales
- Discrete - fine structure
- Numerical stability

IDE solver

- Adding new features is trivial: GW radiation, particle production, etc...
- Accurate on large scales
- Fast and in finite time
- Access to full distribution

Conclusion

- Observations are already here and will be more and more precise
- There are tensions in our current approach to cosmic string predictions
- There are hints that fragmentation may play a role
- Built a consistent (though idealized) model of fragmentation and numerical techniques to solve it
- ULM and IDE are complementary (consistency check, scaling VS non-scaling...)

Conclusion

- Observations are already here and will be more and more precise
- There are tensions in our current approach to cosmic string predictions
- There are hints that fragmentation may play a role
- Built a consistent (though idealized) model of fragmentation and numerical techniques to solve it
- ULM and IDE are complementary (consistency check, scaling VS non-scaling...)

Next steps

- Calibrate $\mathcal{B}$ on NG simulations
- Comparison with NG and AH simulations

Thank you

Cosmic string interpretation: NANOGRAV

- NANOGRAV seems to favor Superstrings but...

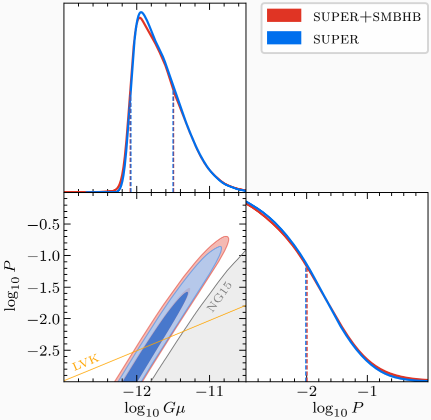

Figure: Afzal et al. 2023

Cosmic string interpretation: NANOGRAV

- NANOGRAV seems to favor Superstrings but...
- $\Omega_{\rm GW}(f) \to \Omega_{\rm GW}(f)/P$

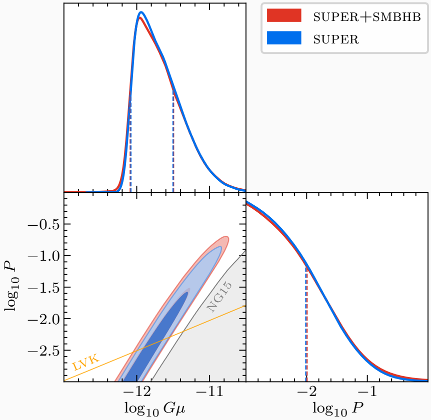

Figure: Afzal et al. 2023

Cosmic string interpretation: NANOGRAV

- NANOGRAV seems to favor Superstrings but...
- $\Omega_{\mathrm{GW}}(f) \to \Omega_{\mathrm{GW}}(f)/P$
- Not a detection of P

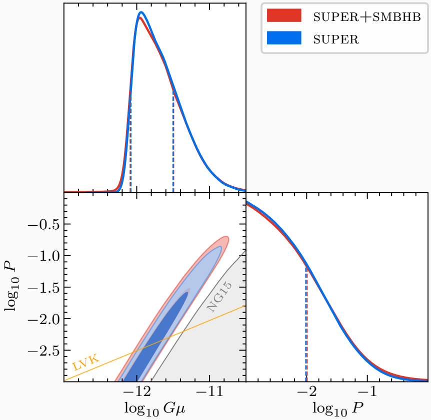

Figure: Afzal et al. 2023

Cosmic string interpretation: NANOGRAV

- NANOGRAV seems to favor Superstrings but...
- $\Omega_{\mathrm{GW}}(f) \to \Omega_{\mathrm{GW}}(f)/P$
- Not a detection of P
- Not a detection with SMBHB

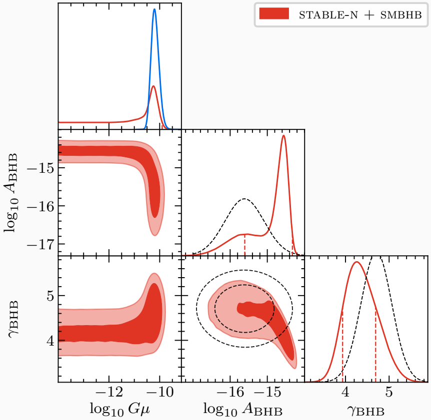

Figure: Afzal et al. 2023

Cosmic string interpretation: NANOGRAV

- NANOGRAV seems to favor Superstrings but...
- $\Omega_{\rm GW}(f) \to \Omega_{\rm GW}(f)/P$
- Not a detection of P
- Not a detection with SMBHB

$$\text{BOS model} = \begin{cases} \text{STABLE-C} & \text{Only cusp emission} \\ \text{STABLE-K} & \text{Only kink emission} \\ \text{STABLE-M} & \text{Only fundamental mode} \\ \text{STABLE-N} & \text{Numerical GW emission} \\ \text{SUPER} & \text{Factor } 1/P \end{cases}$$

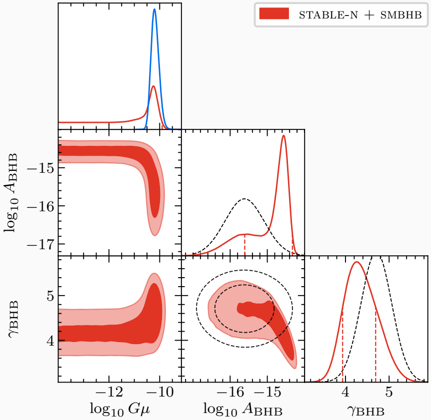

Figure: Afzal et al. 2023

Cosmic string interpretation: EPTA

- EPTA studied the BOS[a] and the LRS[b] models

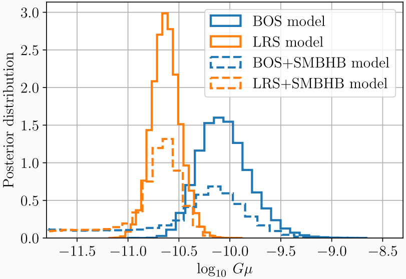

Figure: Antoniadis et al. 2023

[a] Jose J. Blanco-Pillado, Olum, and Shlaer 2014.
[b] Lorenz, Ringeval, and Sakellariadou 2010.
[c] Quelquejay Leclere et al. 2023.

Cosmic string interpretation: EPTA

- EPTA studied the BOS[a] and the LRS[b] models
- Values of $G\mu$ are comparable for both models

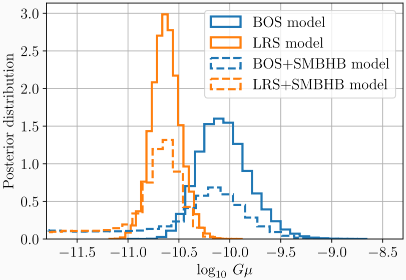

Figure: Antoniadis et al. 2023

[a] Jose J. Blanco-Pillado, Olum, and Shlaer 2014.
[b] Lorenz, Ringeval, and Sakellariadou 2010.
[c] Quelquejay Leclere et al. 2023.

Cosmic string interpretation: EPTA

- EPTA studied the BOS[a] and the LRS[b] models
- Values of $G\mu$ are comparable for both models
- EPTA does not favor a model in particular with $\mathcal{B} \approx 0.3$[c]

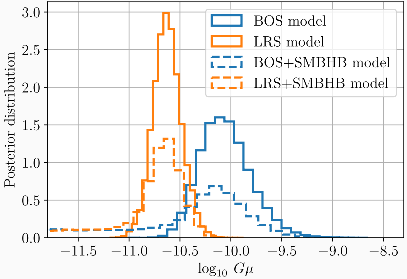

Figure: Antoniadis et al. 2023

[a] Jose J. Blanco-Pillado, Olum, and Shlaer 2014.
[b] Lorenz, Ringeval, and Sakellariadou 2010.
[c] Quelquejay Leclere et al. 2023.

What is the deal with Nambu-Goto models?

Model LRS

Lorenz, Ringeval, Sakellariadou (2010)

- Loop number density of all loops

Cosmological evolution of cosmic string loops 7

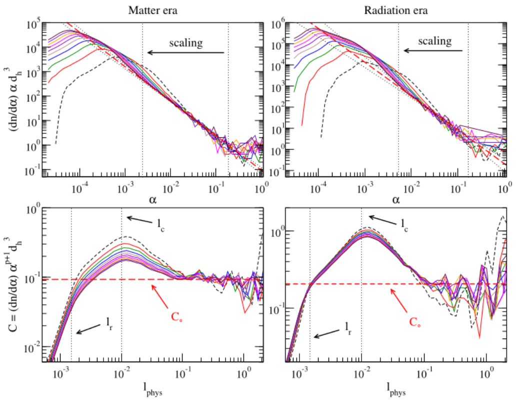

Model LRS

Lorenz, Ringeval, Sakellariadou (2010)

- Loop number density of all loops
- Analytical model of Polchinski-Rocha

2.2. Loop production function

The scaling law of Eq. (1) implies that, once the scaling regime is reached, $t^4\mathcal{F}(\gamma,t)$ should be a function of γ only. From Eq. (12), we expect the same to happen for $t^5\mathcal{P}(\gamma,t)$. Following Refs. [55, 56, 59], we moreover assume that this function is a power law, namely

$$t^5\mathcal{P}(\gamma,t) = c\,\gamma^{2\chi-3}\,, \tag{13}$$

where c and χ are two parameters that will be fixed to fit Eq. (2). However, according to our discussion of Sec. 1, the above expression is only valid for a range of γ values where gravitational backreaction effects can be neglected. Hence, Eq. (13) holds for values of γ greater than

$$\gamma_{\mathrm{c}} \equiv \frac{\alpha_{\mathrm{c}}}{1-\nu} \simeq \Upsilon(GU)^{1+2\chi}, \tag{14}$$

where Υ is a number $\mathcal{O}(10)$ [50]. The parameter χ in this expression is expected to be the same as in Eq. (13), given that the gravitational backreaction length scale is precisely derived from the same two-point correlators used in the PR model to obtain Eq. (13) (see Ref. [50]). In our phenomenological approach, we consider γ_{c} as a free

Model LRS

- Loop number density of all loops
- Analytical model of Polchinski-Rocha
- Matching on the loop number density

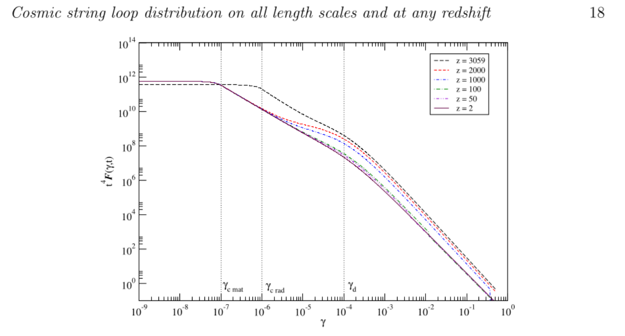

Model LRS

Lorenz, Ringeval, Sakellariadou (2010)

- Loop number density of all loops
- Analytical model of Polchinski-Rocha
- Matching on the loop number density
- 40 ppcl in initial conditions

Caveats

- Small-scales are very model-dependent χ
- Less dynamic range
- "Energy balance"
- "Legacy code"

Cosmic string loop distribution on all length scales and at any redshift 18

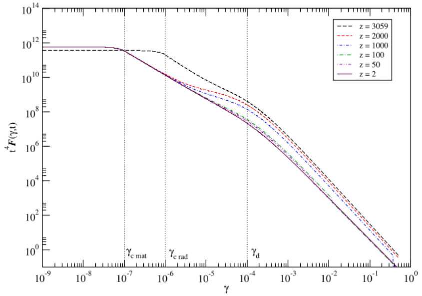

Model BOS

Blanco-Pillado, Olum, Schlaer (2014)

- Loop production function of stable loops

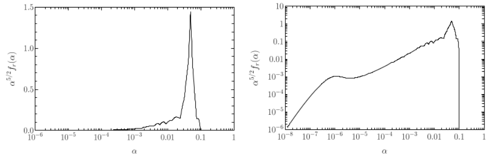

FIG. 2. The loop production rate $f_r(\alpha)$ scaled by $\alpha^{5/2}$, as a function of α on a logarithmic scale. Because $\int \alpha^{3/2} f_r d\alpha = \int \alpha^{5/2} f_r d\ln\alpha$, the area under the curve on the left gives the contribution of each region of α to Eq. (16). The right-hand panel is the same with a logarithmic vertical scale. Notice that the non-scaling peak at $\alpha \sim 10^{-6}$ contributes a negligible fraction of loops.

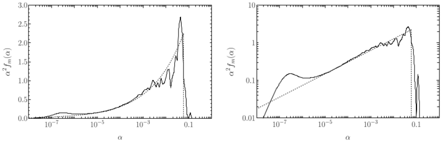

FIG. 8. The loop production rate $f(\alpha)$ scaled by α^2. The non-scaling peak represents a subdominant contribution to the total number of loops, although it may contribute significantly to the small loop sub-population. The dotted line shows the approximation of Eq. (30). Note that the non-scaling peak would be more prominent in these graphs if we were to use the scaling energy instead of the rest mass of the loops. See the corresponding figures in [48]. This is due to the fact that most of the energy of the small loop population is in kinetic energy, not rest mass.

Model BOS

- Loop production function of stable loops
- Analytical model "one-scale model"
- Infer the loop number density

Using Eqs. (16) and (17), and a delta-function approximation for $f_r(\alpha)$ peaked at the typical loop production size $\alpha = 0.05$, we can approximate the loop spectrum by

$$n_r(\alpha) = \frac{0.52\,\Theta(0.05 - \alpha)}{(\alpha + \Gamma G\mu/2)^{5/2}}, \qquad (18)$$

where Θ is the Heaviside step function.

- Loop production function of stable loops
- Analytical model "one-scale model"
- Infer the loop number density
- Also measured the loop number density in (2019)

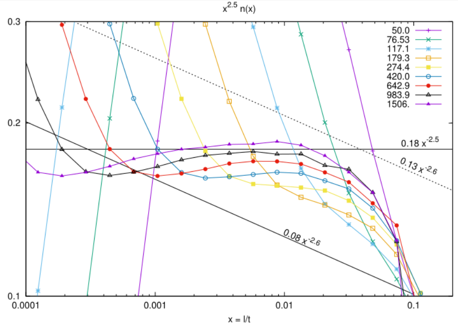

FIG. 1. Loop densities in the radiation era at the conformal times listed, computed from five simulations of size 1500. The scaling loop density has been multiplied by $x^{2.5}$ to make small differences easier to see. The vertical scale ranges only over of a factor of 3 in loop density. Compare with more than 7 orders of magnitude in Fig. 3 of Ref. [16] and 14 orders of magnitude in Fig. 9 of Ref. [19].

Model BOS

- Loop production function of stable loops
- Analytical model "one-scale model"
- Infer the loop number density
- Also measured the loop number density in (2019)

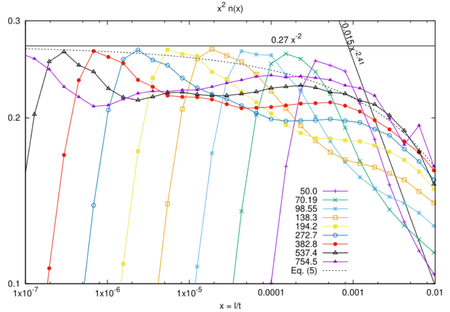

FIG. 2. Loop densities in the matter era at the conformal times listed, computed from two simulations of size 750. The scaling loop density has been multiplied by x^2 to make small differences easier to see. The vertical scale ranges only over of a factor of 3 in loop density, compared with 6 orders of magnitude in Fig. 3 of Ref. [16] and 11 orders of magnitude in Fig. 6 of Ref. [19].

Model BOS

Blanco-Pillado, Olum, Schlaer (2014)

- Loop production function of stable loops
- Analytical model "one-scale model"
- Infer the loop number density
- Also measured the loop number density in (2019)

Caveats

- Small-scales are neglected 1 ppcl
- Fragmentations are neglected
- Scaling is assumed for $t^5\mathcal{P}$

would not have any effect on the network properties. In an expanding universe the situation is complicated by the fact that loops are affected by the cosmological friction, so a non-self-intersecting loop could, in principle, be destabilized and chop itself up, triggering a new stage of fragmentation. We expect this effect to be negligible for any loop of size significantly smaller than the Hubble distance. We have checked that this is not an important effect by letting non-self-intersecting loops oscillate a number of times before being removed. The

Model BOS

Blanco-Pillado, Olum, Schlaer (2014)

- Loop production function of stable loops
- Analytical model "one-scale model"
- Infer the loop number density
- Also measured the loop number density in (2019)

Caveats

- Small-scales are neglected 1 ppcl
- Fragmentations are neglected
- Scaling is assumed for $t^5\mathcal{P}$

Appendix A: Infinitely difficult cosmic string loops

We have identified some new features of Nambu-Goto cosmic strings which are impractical to faithfully simulate. One of these features can be called a "skipping stone." It occurs in particular cases when a network contains a loop which to good approximation is piecewise linear with five or six kinks, and which collides with a long straight segment of string. The collision may occur in such a way as to break off a loop again immediately afterward, one

with less energy but precisely the same shape.

The problem is that the smaller loop will then repeat this process, skipping off the long string again and again, losing energy each time, but never changing shape. Just as a skipping stone leaves behind a geometric series of ripples, this loop will perform (in the Nambu-Goto approximation) an infinite number of intercommutations, leaving behind a geometric series of kinks on the string.

Such a physical process represents a nightmare for a numerical simulation which has no minimum resolution, since each of these ripples will be recorded and evolved.

To avoid the tremendous computational resources required to simulate these rare skipping stones all the way down to the minimum size set by the floating point resolution, we have intentionally failed to perform a certain, very small number of intercommutations. These

Limits

- Matter era is steeper than γ^{-2}

We will compare our results with those of Refs. [16, 20]. Both references claimed that the scaling loop distribution at small x was a power law, which we will write $n(x) = Cx^{-\beta}$. In that notation, Ref. [16] found

$$C = 0.08 \pm 0.05 \qquad \beta = 2.60^{+0.21}_{-0.15} \qquad \text{(radiation)} \tag{1}$$

$$C = (1.5 \pm 0.5) \times 10^{-2} \qquad \beta = 2.41^{+0.08}_{-0.07} \qquad \text{(matter)}\,. \tag{2}$$

Meanwhile, in Ref. [20] we found

$$C = 0.18 \qquad \beta = 2.5 \qquad \text{(radiation)} \tag{3}$$

$$C = 0.27 \qquad \beta = 2.0 \qquad \text{(matter)}. \tag{4}$$

by extrapolating from the loop production function.

Figure: Blanco-Pillado, Olum (2019)

Limits

- Matter era is steeper than γ^{-2}

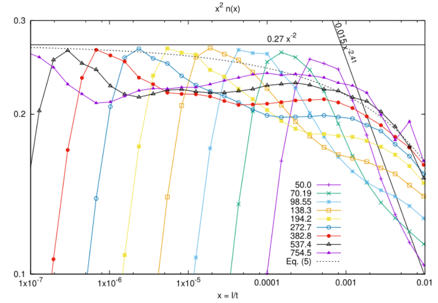

FIG. 2. Loop densities in the matter era at the conformal times listed, computed from two simulations of size 750. The scaling loop density has been multiplied by x^2 to make small differences easier to see. The vertical scale ranges only over of a factor of 3 in loop density, compared with 6 orders of magnitude in Fig. 3 of Ref. [16] and 11 orders of magnitude in Fig. 6 of Ref. [19].

Figure: Blanco-Pillado, Olum (2019)

Limits

- Matter era is steeper than γ^{-2}
- Efficiency factor $\mathcal{F}$ in VOS

lengths at formation. The effect of relaxing this assumption was studied in ref. [95], where it was found that considering a distribution of lengths generally leads to a decrease of the amplitude of the SGWB. To account for this effect, we introduce a second factor, $\mathcal{F}$, which in ref. [101] was estimated to be $\mathcal{O}(0.1)$ for Nambu-Goto strings. Taking these correction factors into account, we rewrite the loop production function in (3.13) as

$$f(x) = \left(\frac{\mathcal{F}}{f_r}\right) \tilde{C} \delta\left(x - \alpha_L \xi\right) \equiv A \ \delta\left(x - \alpha_L \xi\right) . \tag{3.15}$$

[101] J. J. Blanco-Pillado, K. D. Olum and B. Shlaer, Phys. Rev. **D89**, 023512 (2014), [1309.6637], 10.1103/PhysRevD.89.023512.

Figure: Probing the gravitational wave background from cosmic strings with LISA (2019)

Limits

- Matter era is steeper than γ^{-2}
- Efficiency factor $\mathcal{F}$ in VOS
- Disagreement with Field-Theory simulations - how is energy transported to smaller scales

Revised bounds on local cosmic strings from NANOGrav observations

Jun'ya Kume[a,b,c] **and Mark Hindmarsh**[d,e]

completely unknown. In Ref. [53], (a part of) this uncertainty in their distribution was parameterised by allowing a fraction f_{NG} of loops to survive to radiate only gravitationally. Subsequently in Ref. [2], it was assumed that all the AH loops would have the same length distribution as in an NG network $\mathsf{n}(l,t)$, and hence that the distribution of NG-like loops would be $f_{\mathrm{NG}}\mathsf{n}(l,t)$. Then the SGWB from NG-like distribution in the AH string network is quantified as

$$\Omega_{\mathrm{gw}}^{(\mathrm{AH})} = f_{\mathrm{NG}}\Omega_{\mathrm{gw}}^{(\mathrm{NG})}. \tag{2.1}$$

We follow this quantification and discuss possible models of NG loop distributions in the rest of the section.

Results

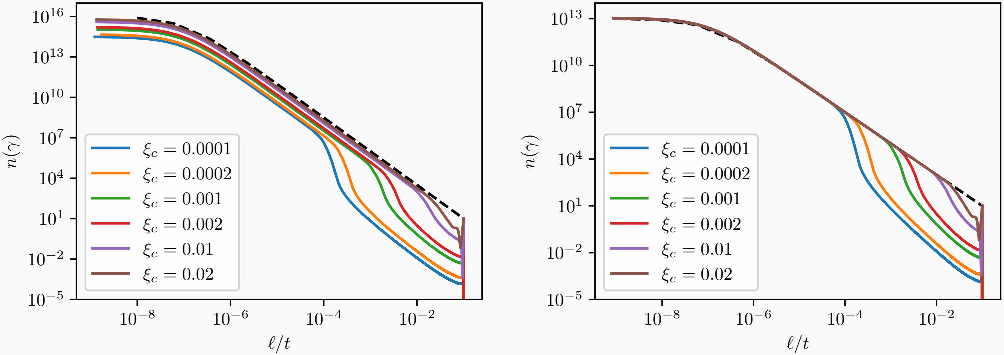

(a) Radiation era **(b)** Matter era

Figure: $(C, \alpha, \chi, \Gamma G\mu, \sigma) = (1, 0.1, 0.2, 10^{-7}, 8)$.

Results

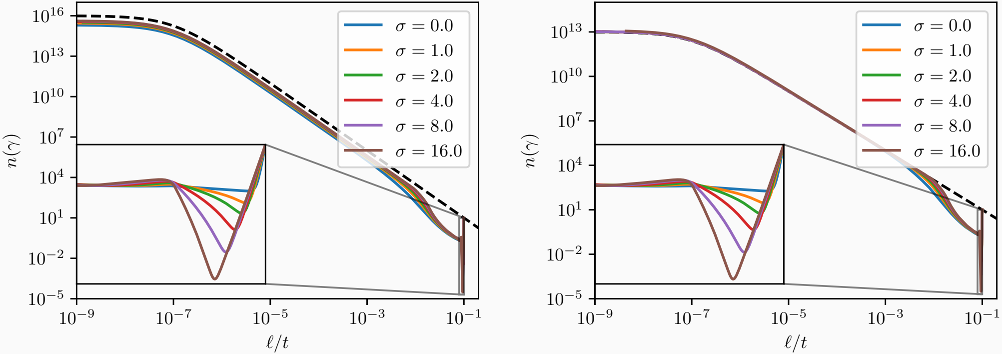

(a) Radiation era

(b) Matter era

Figure: $(C, \alpha, \chi, \nu, \xi_c) = (1, 0.1, 1/2, 10^{-2})$.

Results

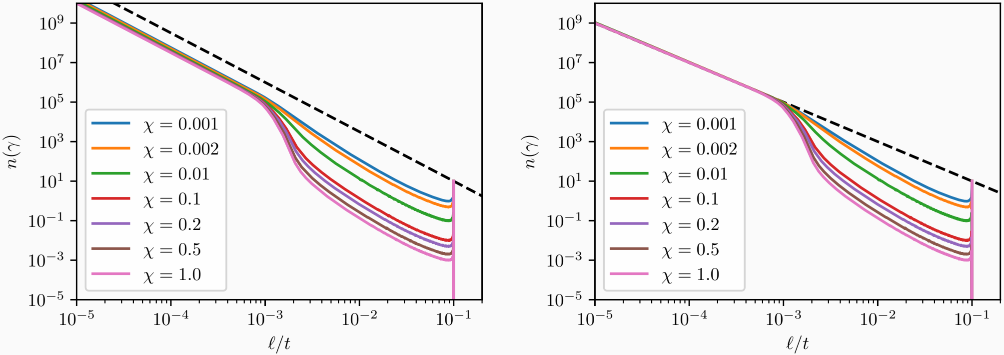

(a) Radiation era

(b) Matter era

Figure: $(C, \alpha, \nu, \Gamma G\mu, \xi_c) = (1, 0.1, 1/2, 10^{-7}, 10^{-3})$.

Asymptotic behavior

Fragmentation limit

Probability to survive

$$G\left(\frac{\ell_\star}{\xi_c}\right) = \exp\left[-\int_{\ell_\star/\alpha}^{\ell_\star/\xi_c} \tau^{-1}\,\mathrm{d}t\right] \underset{\xi_c \ll \alpha}{\approx} \exp\left[-\frac{2\chi\alpha}{\xi_c^{5/2}}\right].$$

$\Longrightarrow$ Fragmentation limit $2\chi\alpha\xi_c^{-5/2} \gg 1$

Asymptotic behavior

Fragmentation limit

Probability to survive

$$G\left(\frac{\ell_\star}{\xi_c}\right) = \exp\left[-\int_{\ell_\star/\alpha}^{\ell_\star/\xi_c} \tau^{-1}\,\mathrm{d}t\right] \underset{\xi_c \ll \alpha}{\approx} \exp\left[-\frac{2\chi\alpha}{\xi_c^{5/2}}\right].$$

$\Longrightarrow$ Fragmentation limit $2\chi\alpha\xi_c^{-5/2} \gg 1$

- Radiation era

$$n(\gamma)\Big|_{\mathrm{rad}} \propto \begin{cases} C\alpha\chi^{-1}\xi_c^{3/2}\gamma^{-5/2} & \gamma \gg \xi_c \\ C\alpha\chi^{-1/4}\xi_c^{3/4}(\gamma + \Gamma G\mu)^{-5/2} & \gamma \ll \xi_c\,. \end{cases}$$

Asymptotic behavior

Fragmentation limit

Probability to survive

$$G\left(\frac{\ell_\star}{\xi_c}\right) = \exp\left[-\int_{\ell_\star/\alpha}^{\ell_\star/\xi_c} \tau^{-1}\,\mathrm{d}t\right] \underset{\xi_c \ll \alpha}{\approx} \exp\left[-\frac{2\chi\alpha}{\xi_c^{5/2}}\right].$$

$\Longrightarrow$ Fragmentation limit $2\chi\alpha\xi_c^{-5/2} \gg 1$

- Radiation era

$$n(\gamma)\Big|_{\mathrm{rad}} \propto \begin{cases} C\alpha\chi^{-1}\xi_c^{3/2}\gamma^{-5/2} & \gamma \gg \xi_c \\ C\alpha\chi^{-1/4}\xi_c^{3/4}(\gamma+\Gamma G\mu)^{-5/2} & \gamma \ll \xi_c\,. \end{cases}$$

- Matter era

$$n(\gamma)\Big|_{\mathrm{mat}} \propto \begin{cases} C\alpha\chi^{-1}\xi_c^{3/2}\gamma^{-5/2} & \gamma \gg \xi_c \\ C\alpha(\gamma+\Gamma G\mu)^{-2} & \gamma \ll \xi_c\,. \end{cases}$$

Impact of the boundary

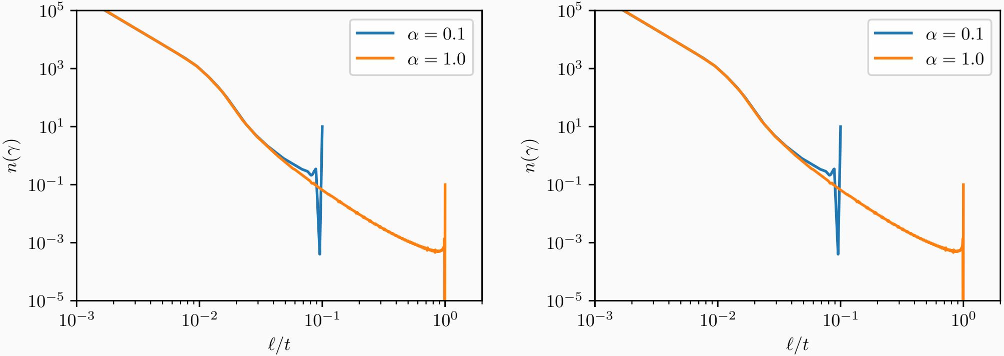

(a) Radiation era

(b) Matter era

Figure: $(\chi, \Gamma G\mu, \xi_c, \sigma) = (0.2, 10^{-7}, 10^{-2}, 8)$

Limits

- Matter era is steeper than γ^{-2}

We will compare our results with those of Refs. [16, 20]. Both references claimed that the scaling loop distribution at small x was a power law, which we will write $n(x) = Cx^{-\beta}$. In that notation, Ref. [16] found

$$C = 0.08 \pm 0.05 \qquad \beta = 2.60^{+0.21}_{-0.15} \qquad \text{(radiation)} \tag{1}$$

$$C = (1.5 \pm 0.5) \times 10^{-2} \qquad \beta = 2.41^{+0.08}_{-0.07} \qquad \text{(matter)}\,. \tag{2}$$

Meanwhile, in Ref. [20] we found

$$C = 0.18 \qquad \beta = 2.5 \qquad \text{(radiation)} \tag{3}$$

$$C = 0.27 \qquad \beta = 2.0 \qquad \text{(matter)}. \tag{4}$$

by extrapolating from the loop production function.

Figure: Blanco-Pillado, Olum (2019)

Limits

- Matter era is steeper than γ^{-2}

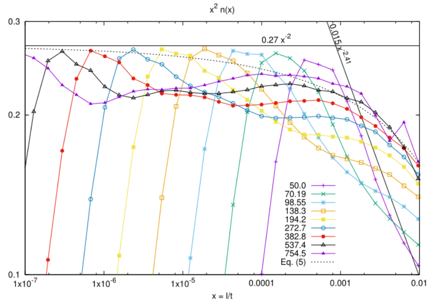

FIG. 2. Loop densities in the matter era at the conformal times listed, computed from two simulations of size 750. The scaling loop density has been multiplied by x^2 to make small differences easier to see. The vertical scale ranges only over of a factor of 3 in loop density, compared with 6 orders of magnitude in Fig. 3 of Ref. [16] and 11 orders of magnitude in Fig. 6 of Ref. [19].

Figure: Blanco-Pillado, Olum (2019)

Limits

- Matter era is steeper than γ^{-2}
- Efficiency factor $\mathcal{F}$ in VOS

lengths at formation. The effect of relaxing this assumption was studied in ref. [95], where it was found that considering a distribution of lengths generally leads to a decrease of the amplitude of the SGWB. To account for this effect, we introduce a second factor, $\mathcal{F}$, which in ref. [101] was estimated to be $\mathcal{O}(0.1)$ for Nambu-Goto strings. Taking these correction factors into account, we rewrite the loop production function in (3.13) as

$$f(x) = \left(\frac{\mathcal{F}}{f_r}\right) \tilde{C}\delta\left(x - \alpha_L \xi\right) \equiv A\ \delta\left(x - \alpha_L \xi\right)\ . \tag{3.15}$$

[101] J. J. Blanco-Pillado, K. D. Olum and B. Shlaer, Phys. Rev. **D89**, 023512 (2014), [1309.6637], 10.1103/PhysRevD.89.023512.

Figure: Probing the gravitational wave background from cosmic strings with LISA (2019)

Limits

- Matter era is steeper than γ^{-2}
- Efficiency factor $\mathcal{F}$ in VOS
- Disagreement with Field-Theory simulations - how is energy transported to smaller scales

Revised bounds on local cosmic strings from NANOGrav observations

Jun'ya Kume[a,b,c] **and Mark Hindmarsh**[d,e]

completely unknown. In Ref. [53], (a part of) this uncertainty in their distribution was parameterised by allowing a fraction $f_{\rm NG}$ of loops to survive to radiate only gravitationally. Subsequently in Ref. [2], it was assumed that all the AH loops would have the same length distribution as in an NG network $\mathsf{n}(l,t)$, and hence that the distribution of NG-like loops would be $f_{\rm NG}\mathsf{n}(l,t)$. Then the SGWB from NG-like distribution in the AH string network is quantified as

$$\Omega_{\rm gw}^{\rm (AH)} = f_{\rm NG}\Omega_{\rm gw}^{\rm (NG)}. \tag{2.1}$$

We follow this quantification and discuss possible models of NG loop distributions in the rest of the section.